Effect of shock pulse width on the shock response of small form factor disk drives

Puneet Bhargava and David B. Bogy

Computer Mechanics Laboratory

Department of Mechanical Engineering

University of California at Berkeley

Berkeley, CA 94720

Telephone: (510) 642-4975

Fax: (510) 643-9786

puneet@cml.berkeley.edu

January 5, 2006

Contents

1 Introduction **1**

1.1 Motivation 1

1.2 Methodology 1

1.3 Prior Work 2

2 Component Dynamics **3**

2.1 Disk 4

2.2 Suspension 5

3 Simulations **5**

3.1 Procedure 5

3.2 Results and Discussion 6

4 Conclusions **8**

5 Tables **11**

6 Figures **12**

List of Figures

1 Half-sine shock pulse 12

2 The disk umbrella mode 12

3 Disk response for 200G shock of varying pulse widths 13

4 Maximum disk deflection for 200G shock of varying pulse widths 13

5 Disk response spectra for 200G shock of varying pulse widths 14

6 Suspension schematic 14

7 Suspension first bending mode 15

8 Suspension first torsion mode 15

9 Suspension second bending mode 15

10 Suspension response to a 200G shock of varying pulse widths 16

11 Suspension response spectra for a 200G shock of varying pulse widths 16

12 Structural Air-bearing coupling scheme 17

13 Slider Design 18

14 Slider Response for 125G, 0.2ms shock 19

15 Frequency spectra of load beam and disk response to 125G, 0.2ms shock . . 20

16 Dimple, limiter status for 125G, 0.2ms shock 21

17 Air bearing and contact forces for 125G, 0.2ms shock 22

18 Slider Response for 250G, 0.5ms shock 23

19 Slider Response for 375G, 1.0 ms shock 24

20 Slider Response for 400G, 1.0 ms shock 25

21 Dimple, limiter status for 400G, 1.0 ms shock 26

22 Slider Response for 400G, 2.0 ms shock 27

23 Slider Response for 450G, 3.0 ms shock 28

24 Safe shock levels for varying pulse widths 29

List of Tables

1 Disk parameters 11

2 Slider parameters 11

Abstract

This paper discusses the effect of varying the shock pulse width on the shock response of small form factor hard disk drives. We develop a new shock simulator for hard disk drives which simulates the Structural as well as the air bearing dynamics of the disk drive simultaneously. We observe that the response of the disk to the shock pulse is of critical importance and depends strongly on the pulse width of the shock pulse. We also find that if a suspension bending frequency is close to the first umbrella frequency of the disk, there can be failure of the head-disk interface due to resonance.

1 Introduction

1.1 Motivation

Recently there has been an increased interest in the effect of shocks on hard disk drives due their increased usage in hostile environments. Over the past few years an increase in the demand of storage capacity in small consumer appliances and gadgets such as MP3 players, cameras and cell phones has led to the application of small form factor hard disk drives in these devices. Due to the hostile environments faced by such devices, the shock resistance of these small form factor drives has become of great importance.

1.2 Methodology

Zeng and Bogy (2000) mentioned that there are essentially three approaches for dealing with shock problems. The first being the design and installation of a suitable isolation system for the disk drives. The second, to design a robust servo control mechanism to prevent read/write errors during shock and the third is to design a robust mechanical system such that the head-disk interface is resistant to shock. The combination of these three techniques needs to be used to effectively counter the problem of shock.

In this paper we study the mechanism of failure of the head-disk interface during shock. We develop a shock simulator to accurately simulate the shock event and predict the response of the suspension-slider-disk system. This simulator is used to simulate the shock response of a system for various different kinds of shock, which are characterized by varying pulse widths for their acceleration pulse. This allows us to simulate drops on surfaces of varying stiffness. We simulate shocks of pulse widths from 0.2 ms to 3.0 ms. A shock of 0.2 ms could correspond to the disk-drive falling on a concrete pavement (depending on the amount of shock isolation provided in the drive) and 3.0 ms could corrspond to the drive falling on a carpeted floor. As we increase the pulse width of the shock the response tends to become more quasi static in nature, with the acceleration pulse leading simply to a gram load change for the air bearing, but with little dynamic effects. Hence we limit the study to a maximum pulse width of 3.0 ms.

1.3 Prior Work

Over the past few years there have been various experimental and simulation studies on the shock response of the mechanical system and its effects on the head-disk interface. Many of these studies (Harrison and Mundt (2000), Edwards (1999), Kumar et al. (1994), Kouhei et al. (1995)) have been limited to the non-operating state of the drives, and/or to the component level. Various other papers (Jayson et al. (2003), Jiang et al. (1995)) have considered shock simulations in the operating state using simplified models for one or more components of the drive, i.e. either the disk,suspension or the air bearing. A summary of these studies has been presented in Bhargava and Bogy (2005b).

For the simulation of operational shock Zeng and Bogy (2000) proposed a method whereby they separate the simulation work into two essentially uncoupled sets. They developed a finite element model of the disk and suspension system and used it to obtain the dynamic normal load and moments applied to the slider air bearing. These were then used as input data for an air bearing dynamic simulator to calculate the dynamic flying attitudes.

They were able to obtain not only the responses of the structural components, but also the responses of the slider air bearings. Also, simulations where the air bearing exhibits highly nonlinear behavior, such as when the air bearing collapses, may require iterations between the structural and air bearing simulations, thereby making the process cumbersome and computationally more expensive. In a previous paper, Bhargava and Bogy (2005b) proposed a method where the modeling of the structural components was done in ANSYS, a commercial finite elment package. The air bearing modeling was done using the CML dynamic air bearing simulator. The two modules are coupled and each is iterated to convergence at every time step. The pulse width of the shock was kept constant at 0.5 ms and the magnitude of the shock pulse was varied. However, this method was inefficient and computationally expensive due to the exchange of data between the two modules at each time step.

In this paper we propose an improved simulation method whereby the structural modeling module is transferred into the air bearing code using preassembled exported mass and stiffness matrices from ANSYS. This method is found to be as accurate, though much faster and robust, than the one proposed earlier. Using the new simulator, we simulate the effect of the pulse width on the shock resistance of a 1" drive.

In the following sections we start with a discussion on the dynamics of the individual structural components, i.e. the disk and the suspension, followed by a presentation of our simulation results and an explanation of those results based on the dynamics of the individual components, followed by conclusions and remarks at the end of the paper.

2 Component Dynamics

In this section we discuss the dynamics and the shock response of the main structural components of the disk drive, i.e. the disk and the suspension.

2.1 Disk

To study the effect of the shock pulse width on the response of the disk drive, we first study the response of the disk to shocks of varying pulse widths (see Figure 1 for a description of the shock pulse). The parameters of the disk are given in Table 1. It has been shown in various studies (Zeng and Bogy (2000), Bhargava and Bogy (2005b)) that the shock response of a rotating disk to an axisymmetric shock is primarily composed of the first umbrella mode (Figure 2). The only effect of the rotation of the disk on the umbrella modes is due to centrifugal stiffening. For low speeds of rotation, such as 3600 RPM, and small diameters of the disk, this effect is negligible and hence the disk can be modeled as stationary for these cases. The z-displacement of a point on the OD of the disk, when subject to an acceleration pulse of 200G magnitude and varying pulse width is plotted in Figure 3. We observe that even thought the magnitude of the acceleration impulse is 200G in each case, the response of the disk is very different for different pulse widths. We observe that for a short pulse width like 0.2 ms, much more energy is transferred to the disk than for a pulse width like 0.5 ms. The maximum amplitudes during the shock and during the post-shock response of the disk are plotted in Figure 4. We see that the deflection in the post-shock response of the disk is a strong function of the pulse width of the shock. For example, with a pulse width of 0.5 ms, even though the disk might deflect more than 6 μm during the shock, the disk only oscillates at less than 0.5 μm after the shock. However for a pulse width of 0.2 ms the disk deflection during and after the shock both are large. We will see that such large disk oscillations in the post-shock stage can lead to failure of the head-disk interface due to resonance with the suspension. Figure 5 shows a waterfall plot of the frequency spectra of the disk response to a 200G shock of varying pulse widths. We see that the primary mode excited in all cases, is the first umbrella mode (see Figure 2) at 3.04 KHz. However, the amount of power in this mode varies stongly with the pulse width, as also seen in Figure 4.

2.2 Suspension

The suspension is one of the most important structural components in the hard disk drive. A schematic diagram of the suspension is shown in Figure 6. In a 1" drive, the suspension attaches directly to the actuator hub.

For the simulations we used a suspension model from a popular 1" drive. The first three suspension modes of vibration, the first and second bending modes and the first torsion mode, are plotted in Figures 7 - 9. We see that the frequency of the second bending mode, shown in Figure 9, is 3.12 KHz, which is very close to the umbrella mode of vibration of the disk. In Figure 10 we plot the free suspension shock response (displacement of slider center) to a 200G shock of varying pulse widths. In Figure 11 we plot the power spectra of these responses. We see that the primary mode of vibration for all pulse widths is the first bending mode, with a frequency of 320.6 Hz. For a pulse width of 0.2 ms there is also some power in the second bending mode, which is at around 3.12 KHz. However, we will see that when the suspension is loaded onto the disk, the second bending mode can get excited due to resonance with the umbrella mode of the disk, which can lead to failure of the head-disk interface.

3 Simulations

3.1 Procedure

A new simulator was developed to simulate the shock response of the suspension-slider-disk system. The simulator models the reponse of the structural components (i.e. the disk and the suspension) as well as the slider air bearing. The structural components are modeled using finite elements. These are incorporated in the form of matrices for mass and stiffness which are preassembled in ANSYS, which is a commercial finite element package. Since the suspension model is very large in size, often of the order of a few hundred thousand degrees

of freedom, we use a technique called 'substructuring' in ANSYS, which is a form of dynamic reduction (see Guyan (1965)). The air bearing is simulated by solving the generalized Reynold's equation using a finite volume implementation (Lu (1997)). The overall structure of the simulator is very similar to what has been previously used by the authors to simulate the load/unload process (see Bhargava and Bogy (2005a)). The structral and air-brearing components of the program are coupled by a fixed point iteration scheme that iterates each module to convergence at each time step. The flowchart for this scheme is shown in Figure 12. In practice, this scheme is found to converge in 1 or 2 iterations, using a time-step of 0.1 μs.

3.2 Results and Discussion

In an earlier report on shock, Bhargava and Bogy (2005b), the authors simulated shocks in + and - z directions, defined as positive and negative shocks, respectively. They showed that positive shocks are much more critical to the head-disk interface. Thus is this report we shall discuss only positive shocks of varying pulse widths.

Various simulations were carried out to investigate the effect of the pulse width on the shock response of the system. In the simulations the slider design used is a 'femco' slider from a poplular 1" disk drive. The design is shown in Figure 13 and its operating parameters are listed in Table 2.

Figure 14 plots the slider attitude response to a 125G shock of 0.2 ms pulse width. The various quantities plotted are, the shock profile in a), the absolute displacement of the slider center, the load/unload (L/UL) tab and the disk in b), the nominal flyheight in c), the minimum clearance in d) and the roll and the pitch in e) and f) respectively. In b), we see that the slider centre follows the displacement of the disk perfectly. However for the L/UL tab, we see that its oscillations (which correspond to the oscillations of the load beam) grow in time, which is due to the resonance between the disk and the suspension. In Figure 15, we see that the frequency of the oscillations of the load beam as well as the disk are close to 3

KHz, which corresponds to the first umbrella mode of the disk and the second bending mode of the suspension. In Figure 14 d), we see that this resonance eventually causes head disk contact. In Figure 16 we plot the contact forces and separations of the dimple and the two limiters (referred to as CE1 and CE2). We can see that as the oscillations of the load beam increase, the dimple begins to open and close repeatedly. Eventually the impacts between the load beam and the flexure become strong enough to cause the slider to contact the disk. The forces corresponding to this response are plotted in Figure 17. In a), we plot the air bearing forces, positive, negative and total and in b) we plot the asperity contact forces (quasi-static, calculated when the flyheight is less than the glide height) and the dynamic impact forces (calculated when the flyheight is less than zero). We see even though there is no impact between the head and the disk during the shock, the resonance in the post-shock response causes severe head disk impact.

In Figure 18, we plot the slider attitude response to a 250G shock of 0.5 ms pulse width. In this case, we see that the oscillations of the load beam (L/UL tab) do not grow in time, since the disk oscillations are weak and insufficient to resonate the suspension. Hence there is no head-disk contact in this case.

In Figure 19, we have plotted the slider attitude response to a 375G shock of 1.0 ms pulse width. We observe that the disk oscillations are strong enough to excite the suspension, however not strong enough to overcome damping and cause head disk contact. Hence we see that eventually the oscillations of both, the disk and the suspension die out.

If we increase the shock to 400G, we see that there is head-disk contact not due to resonance, but because of the shock itself. This is plotted in Figure 20. We see that at about 1.1 ms the load beam which is springing back after being pulled by the shock, hits the flexure and causes the slider to hit the disk. This can be seen from the contact element forces and spacings in Figure 21. We see that just before the slider crashes into the disk, the dimple closes with a large spike in the contact force, which signifies impact.

In Figure 22 and Figure 23, we plot the slider response to shocks of 400G, 2.0 ms and

450G, 3.0 ms, respectively. We see that the head-disk interface is able to withstand larger and larger values of shock at increasing pulse widths. The reason for this is that larger pulse widths lead to lower force gradients and weaker post-shock disk response.

4 Conclusions

We have developed a new shock simulator for disk drives which simultaneously solves the slider air bearing and structural equations to yield the dynamic response of the system to disturbances such as shock. We found that the disk response is critical to the shock resistance of the disk drive. We also found that matching suspension and disk frequencies can lead to resonance and hence failure of the head disk interface. The results of the study are summarized in Figure 24. We plot the 'Safe' shock levels, i.e. the amount of shock the disk drive is able to withstand without head-disk contact as a function of the shock pulse width. We see that for short pulse widths, small magnitudes of shock are sufficient to cause head disk contacts, while for larger pulse widths, the head disk interface is able to withstand much more severe shocks. However, we can avoid short pulse widths during shocks easily by providing a minimal amount of padding/isolation in a space/weight constrained system to increase the shock resistance dramatically even for shocks on the hardest surfaces. We can also avoid resonances between the suspension and the disk by properly designing the suspension such that none of the bending/torsional requencies are close to the disk umbrella frequencies.

Acknowledgment

This study was supported by Seagate Corporation and the Computer Mechanics Laboratory (CML) at the University of California, Berkeley.

References

P. Bhargava and D. B. Bogy. Numerical simulation of load/unload in small form factor hard disk drives. Technical Report 2005-011, CML, University of California, Berkeley, 2005a.

P. Bhargava and D. B. Bogy. Numerical simulation of operational-shock in small form factor hard disk drives. Technical Report 2005-005, CML, University of California, Berkeley, 2005b.

J. R. Edwards. Finite element analysis of the shock response and head slap behavior of a hard disk drive. *IEEE Trans. of Magnetics*, 35:863–867, 1999.

R.J. Guyan. Reduction of stiffness and mass matrices. *AIAA Journal*, 3:310, 1965.

J. C. Harrison and M. D. Mundt. Flying height response to mechanical shock during operation of a magnetic hard drive. *ASME Journal of Tribology*, 122:260–263, 2000.

E. M. Jayson, J. Murphy, P. W. Smith, and F. E. Talke. Shock modeling of the head-media interface in an operational hard disk drive. *IEEE Trans. of Magnetics*, 39:2429–2432, 2003.

Z. W. Jiang, K. Takashima, and S. Chonan. Shock proff design of head disk assembly subjected to impulsive excitation. *JSME International Journal*, 38:411–419, 1995.

T. Kouhei, T. Yamada, Y. Keroba, and K. Aruga. A study of head-disk interface shock resistance. *IEEE Trans. of Magnetics*, 31:3006–3008, 1995.

S. Kumar, V. Khanna, and M. Sri-Jayantha. A study of the head disk interface shock failure. In *The 6th MMM-Intermag Conference*, 1994.

S. Lu. *Numerical Simulation of Slider Air Bearings.* PhD thesis, University of California, Berkeley, 1997.

Q. Zeng and D. B. Bogy. Numerical simulation of shock response of disk-suspension-slider air bearing systems in hard disk drives. Technical Report 2000-003, CML, University of California, Berkeley, 2000.

5 Tables

Table 1: Disk parameters

Parameter	Value
Inner diameter	3.45 mm
Outer diameter	13.68 mm
Thickness	0.38 mm
Young's modulus	75.0 GPa
Density	2.71 g/mm^3
Poisson's ration	0.3

Table 2: Slider parameters

Parameter	Value
Drive form factor	1"
Gram load	1.25 g
RPM	3600
Steady state flyheight (OD)	6.24 nm
Steady state pitch	58.3 μrad
Steady state roll	-2.6 μrad
Operating PSA	2.5 mrad
Operating RSA	0.0 mrad

6 Figures

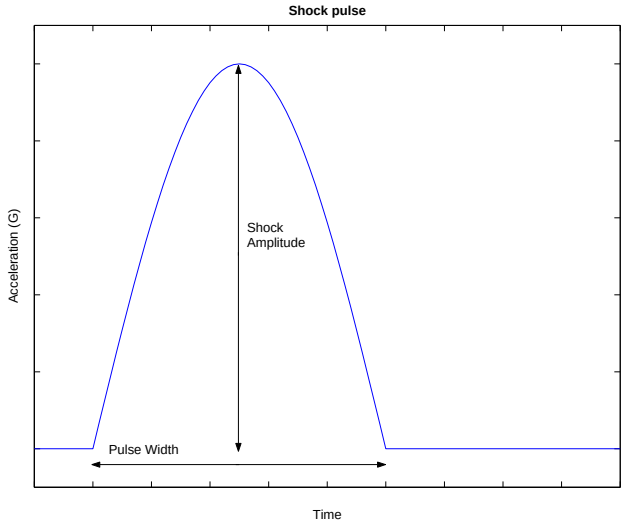

Figure 1: Half-sine shock pulse

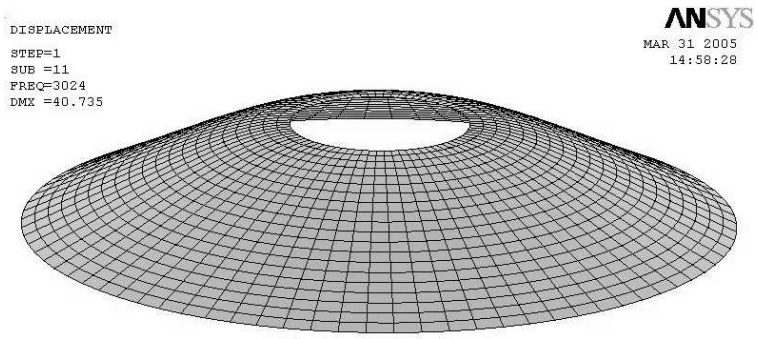

Figure 2: The disk umbrella mode

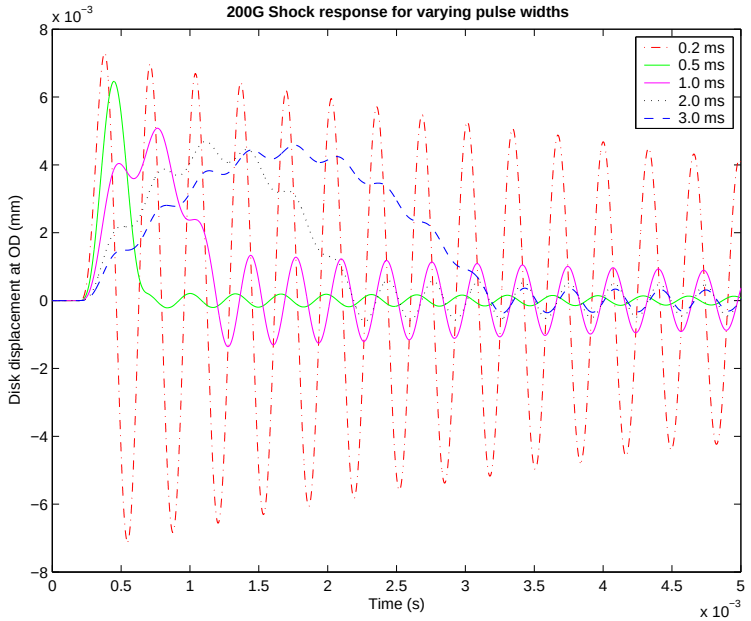

Figure 3: Disk response for 200G shock of varying pulse widths

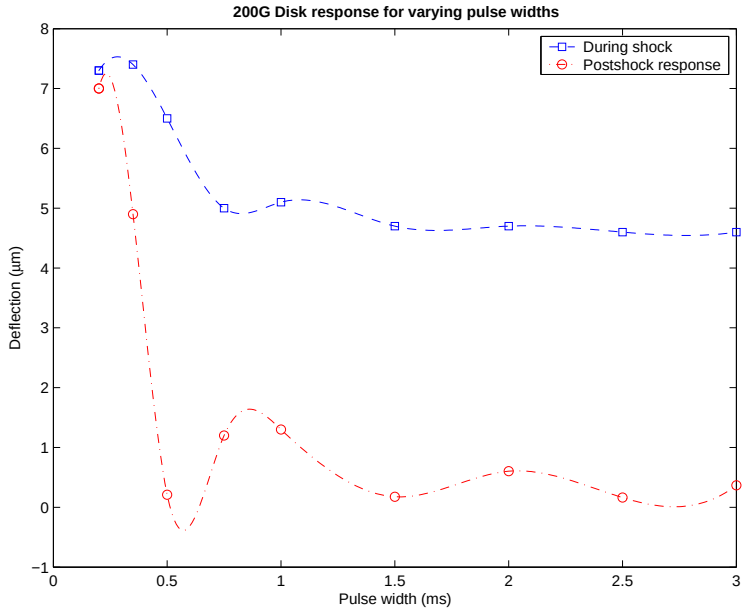

Figure 4: Maximum disk deflection for 200G shock of varying pulse widths

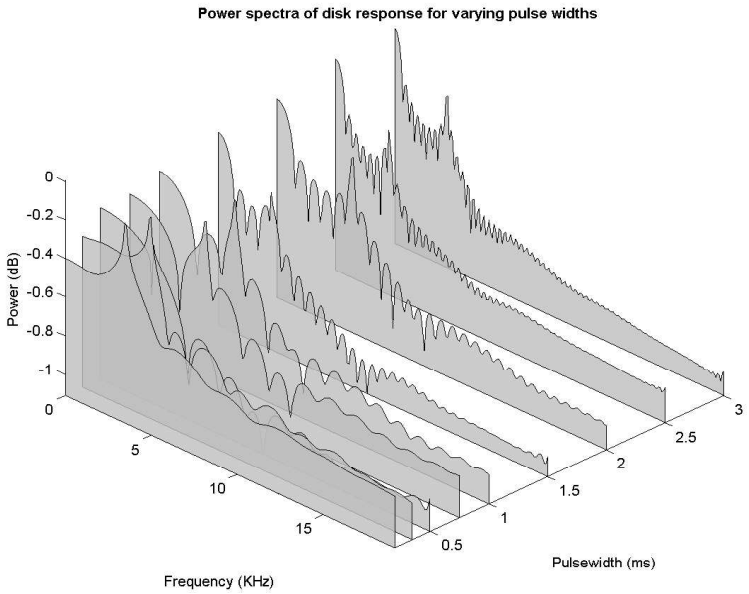

Figure 5: Disk response spectra for 200G shock of varying pulse widths

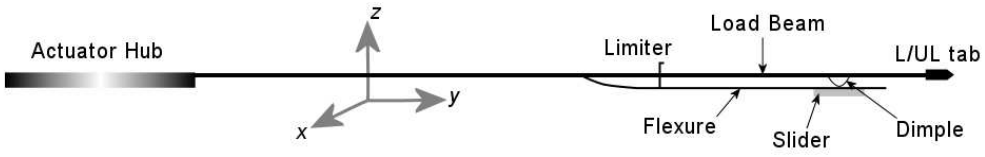

Figure 6: Suspension schematic

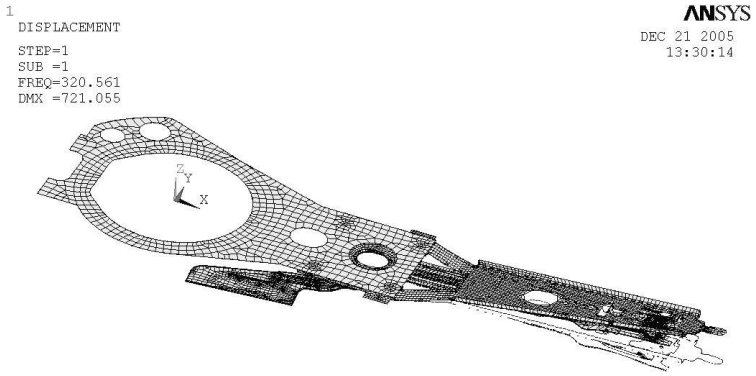

Figure 7: Suspension first bending mode

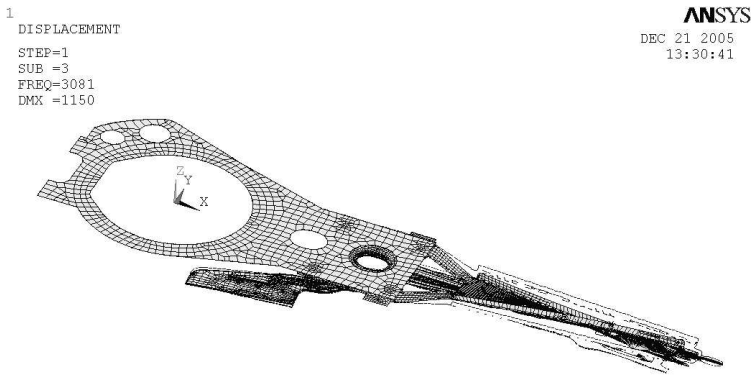

Figure 8: Suspension first torsion mode

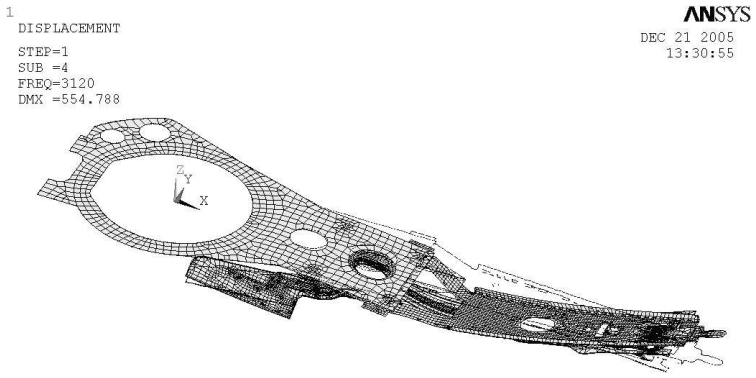

Figure 9: Suspension second bending mode

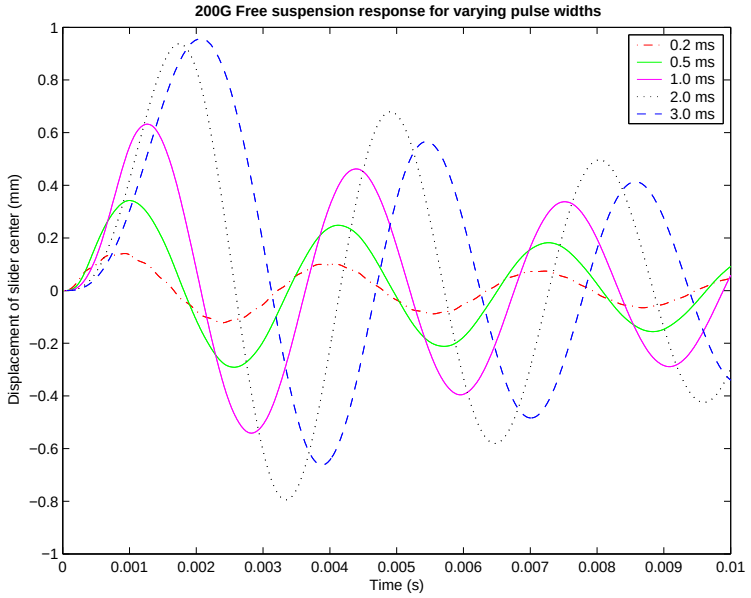

Figure 10: Suspension response to a 200G shock of varying pulse widths

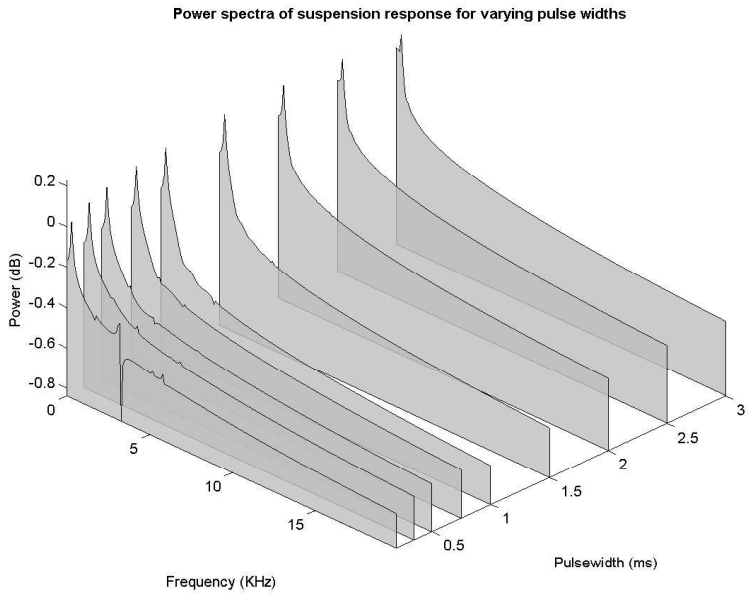

Figure 11: Suspension response spectra for a 200G shock of varying pulse widths

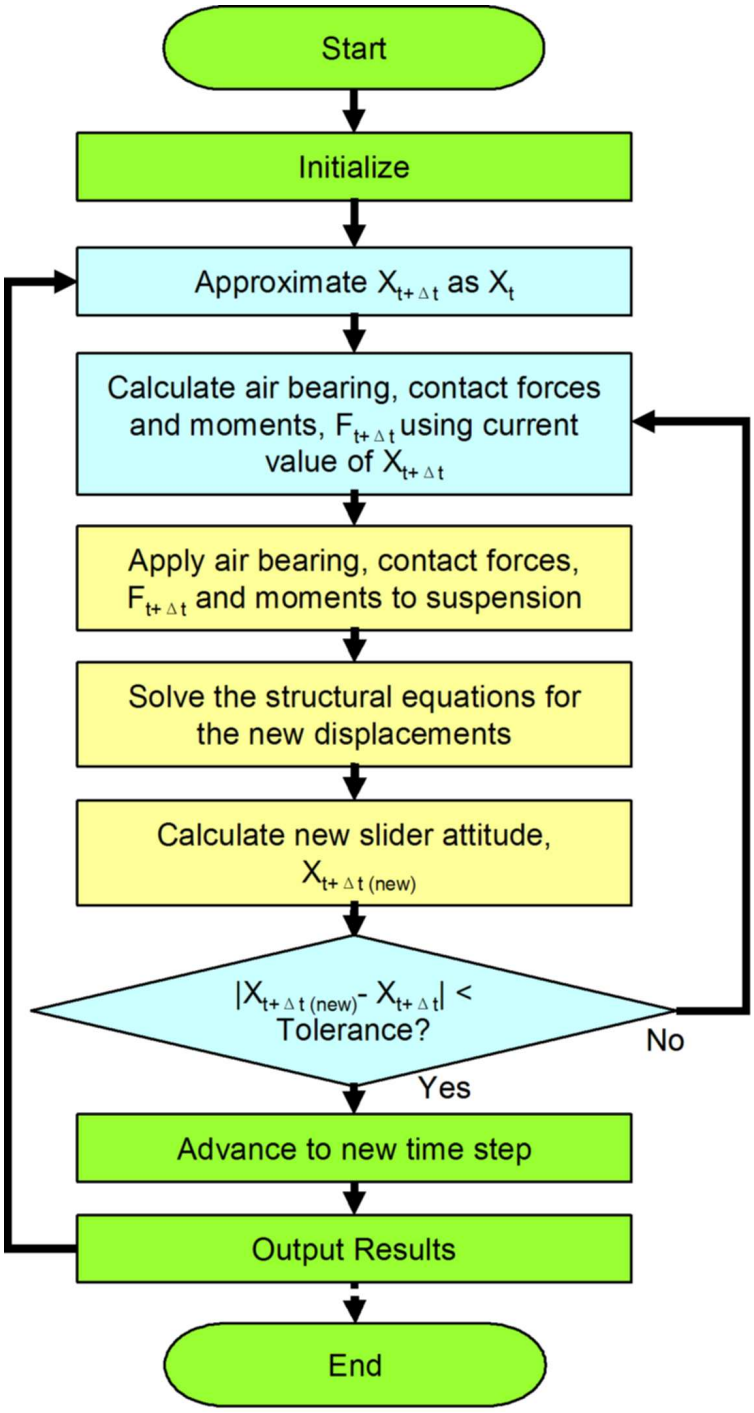

Figure 12: Structural Air-bearing coupling scheme

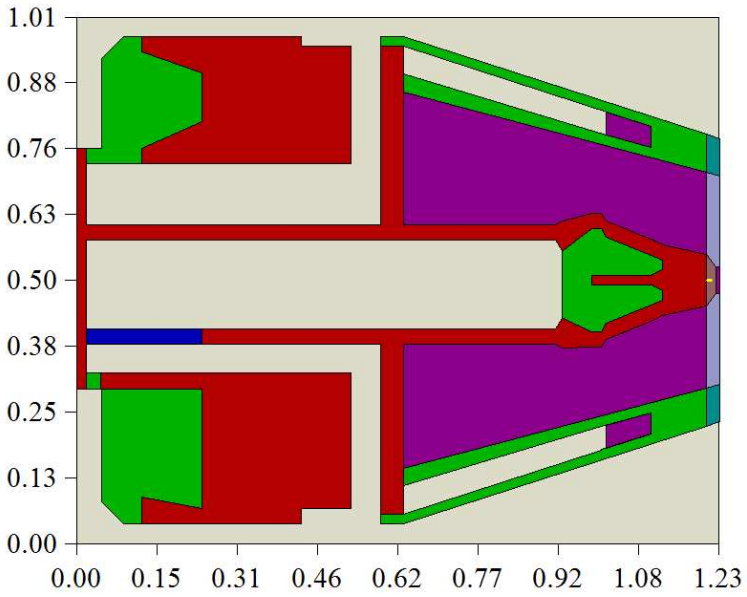

Figure 13: Slider Design

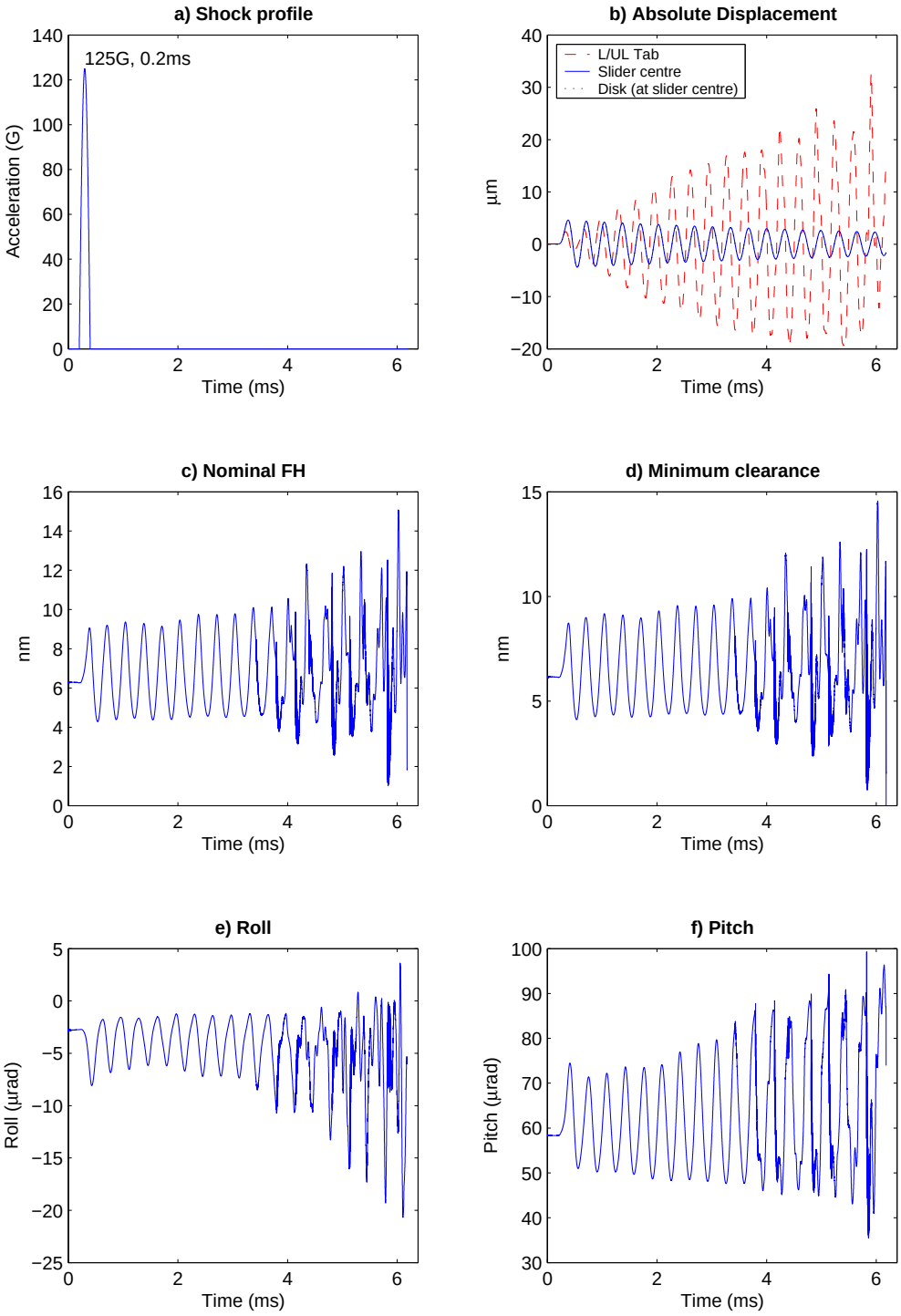

Figure 14: Slider Response for 125G, 0.2ms shock

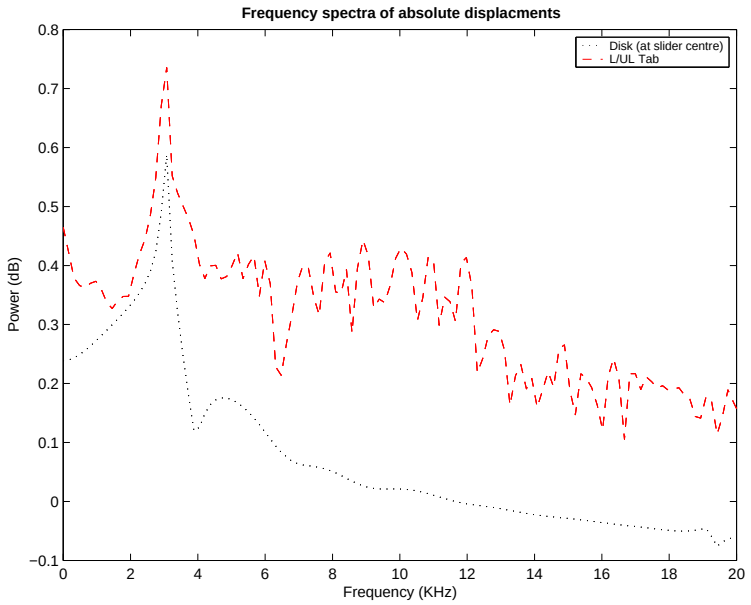

Figure 15: Frequency spectra of load beam and disk response to 125G, 0.2ms shock

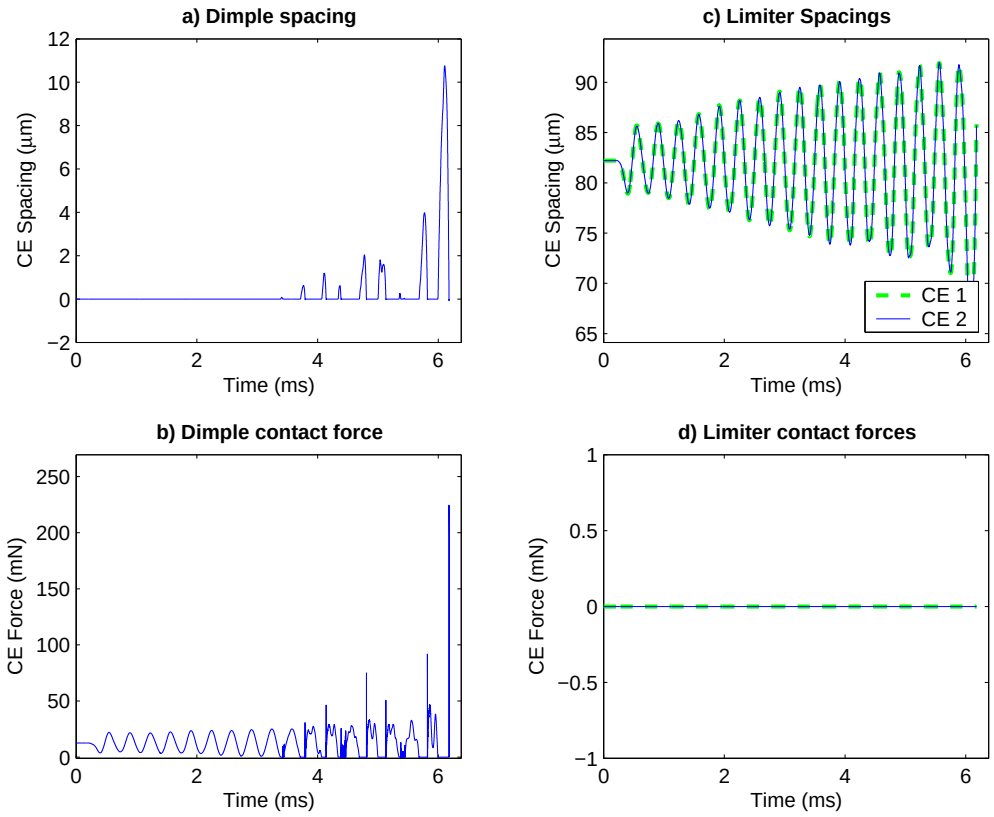

Figure 16: Dimple, limiter status for 125G, 0.2ms shock

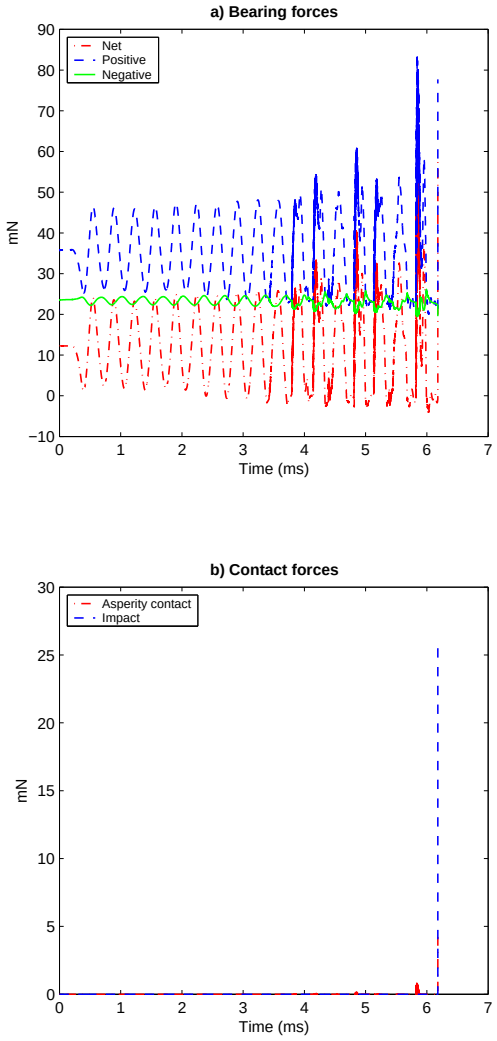

Figure 17: Air bearing and contact forces for 125G, 0.2ms shock

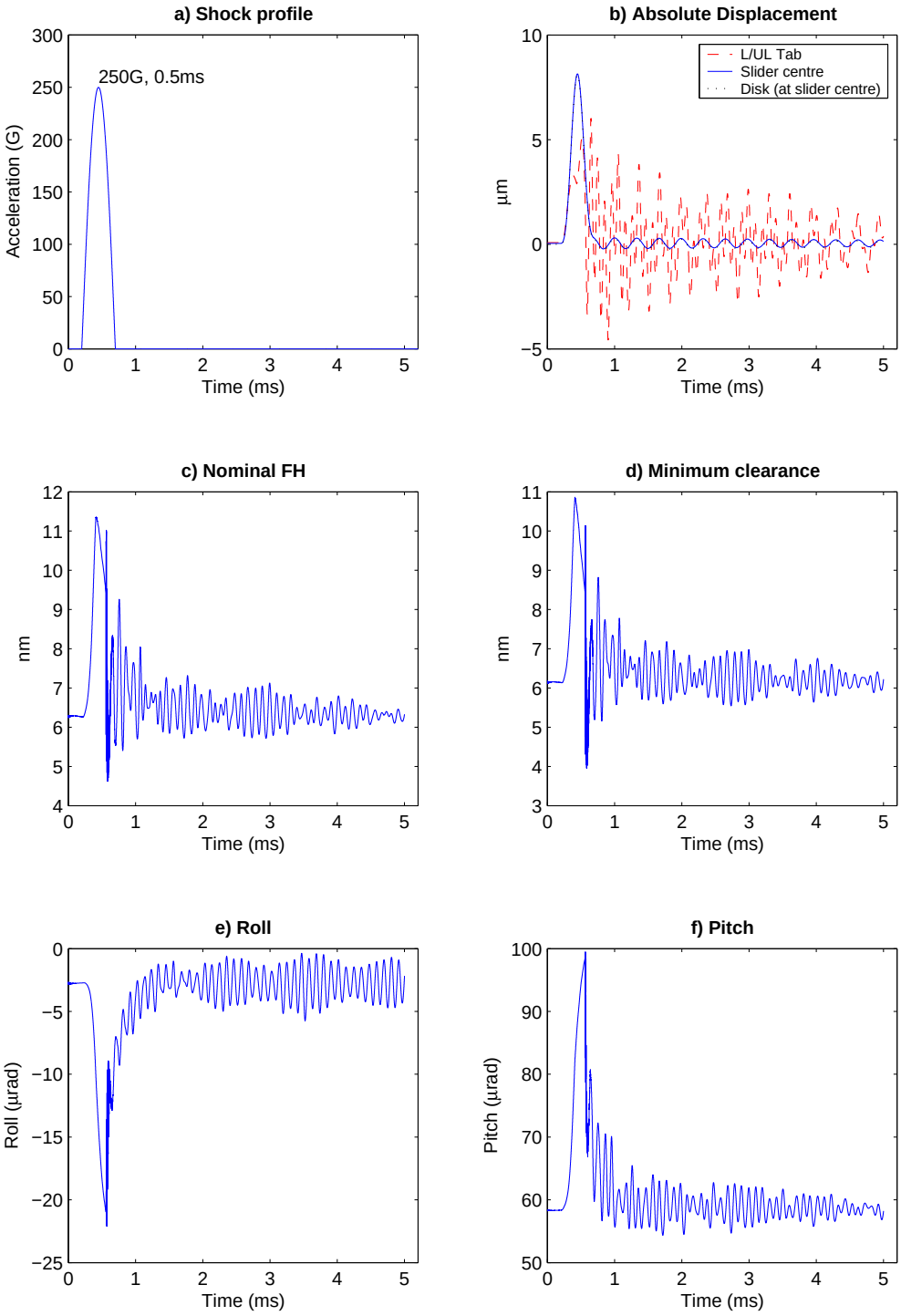

Figure 18: Slider Response for 250G, 0.5ms shock

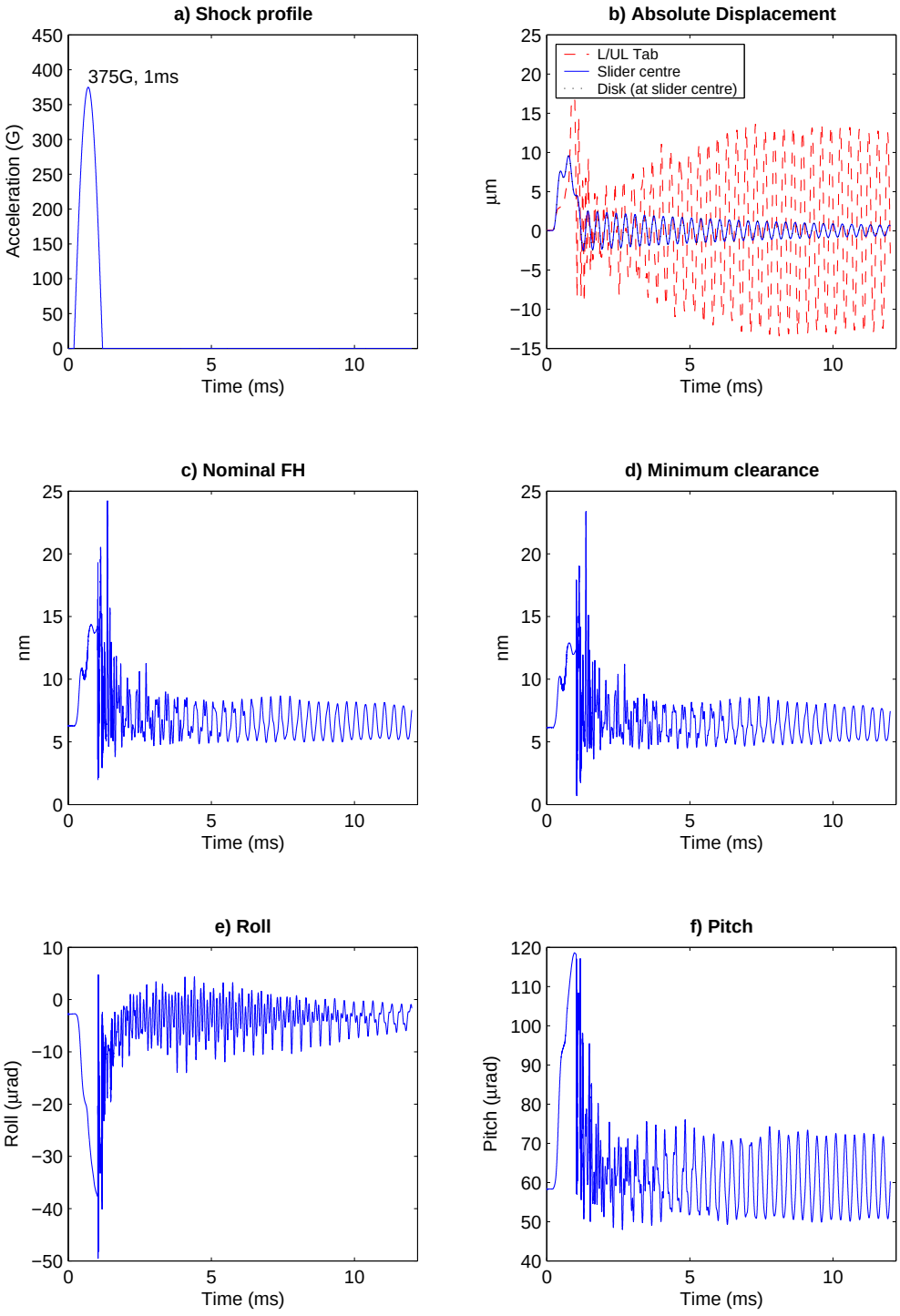

Figure 19: Slider Response for 375G, 1.0 ms shock

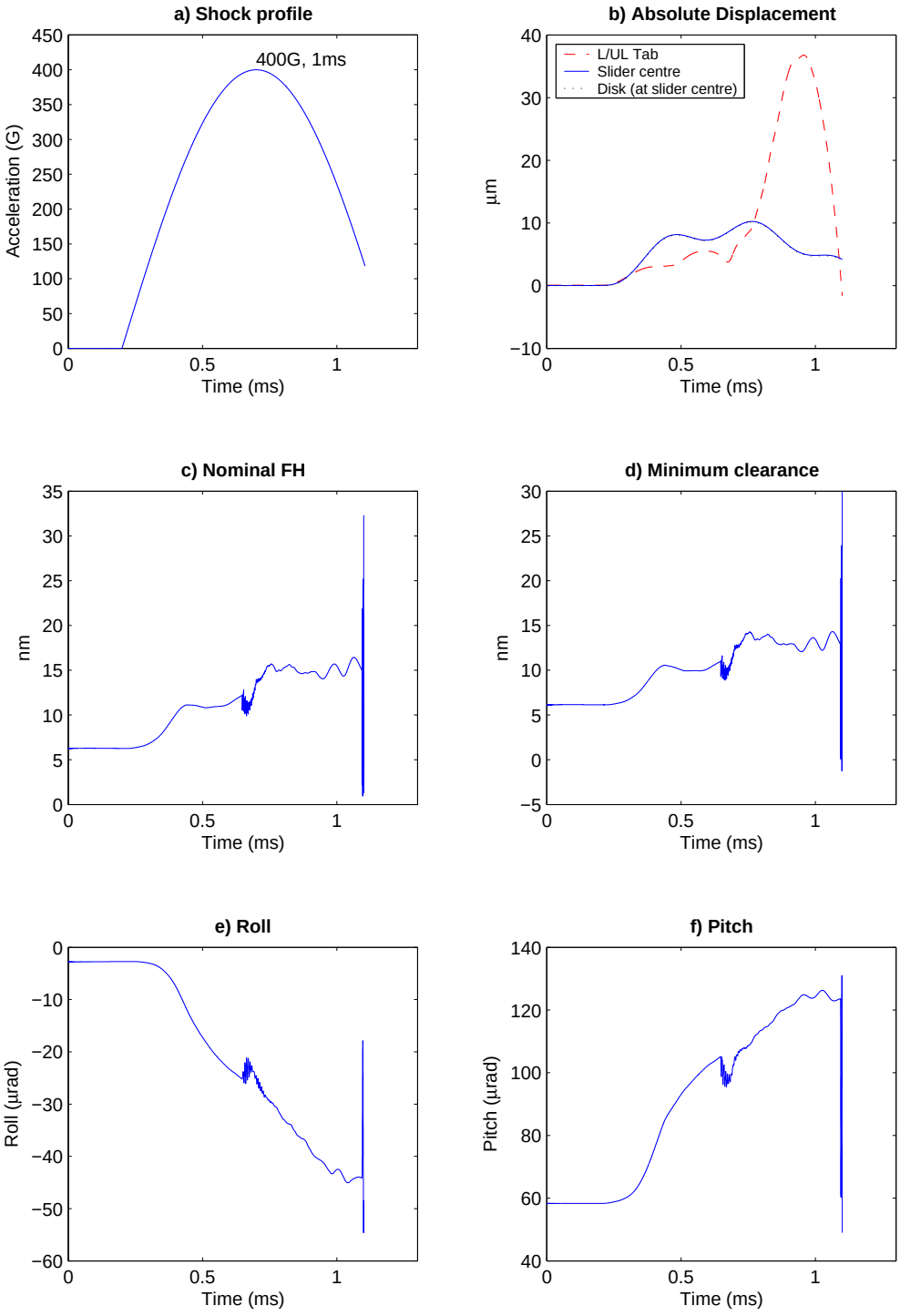

Figure 20: Slider Response for 400G, 1.0 ms shock

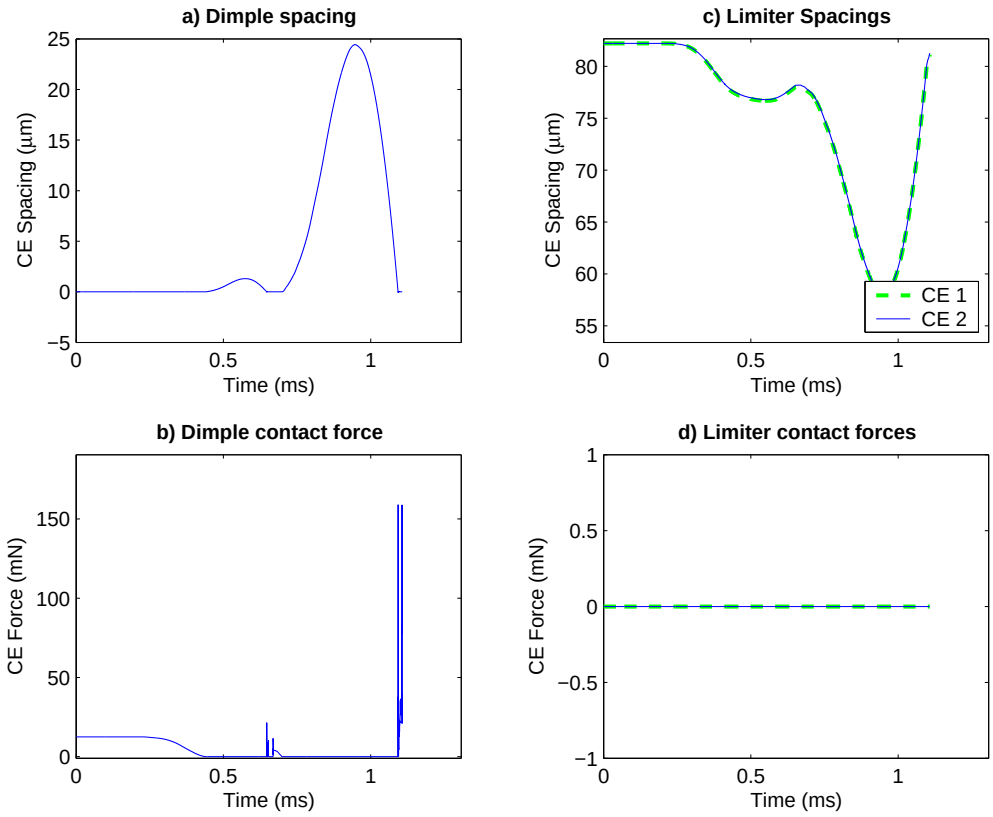

Figure 21: Dimple, limiter status for 400G, 1.0 ms shock

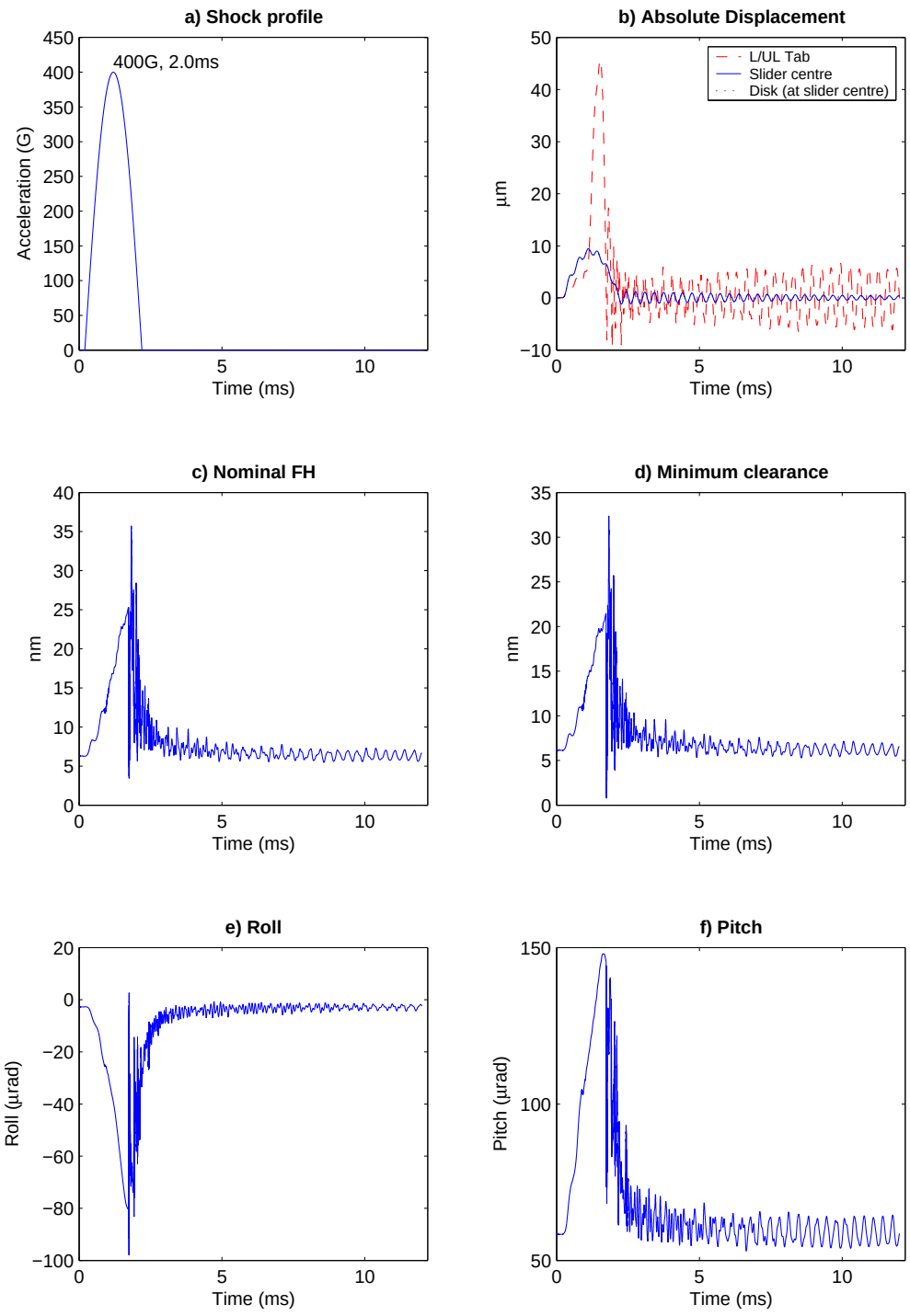

Figure 22: Slider Response for 400G, 2.0 ms shock

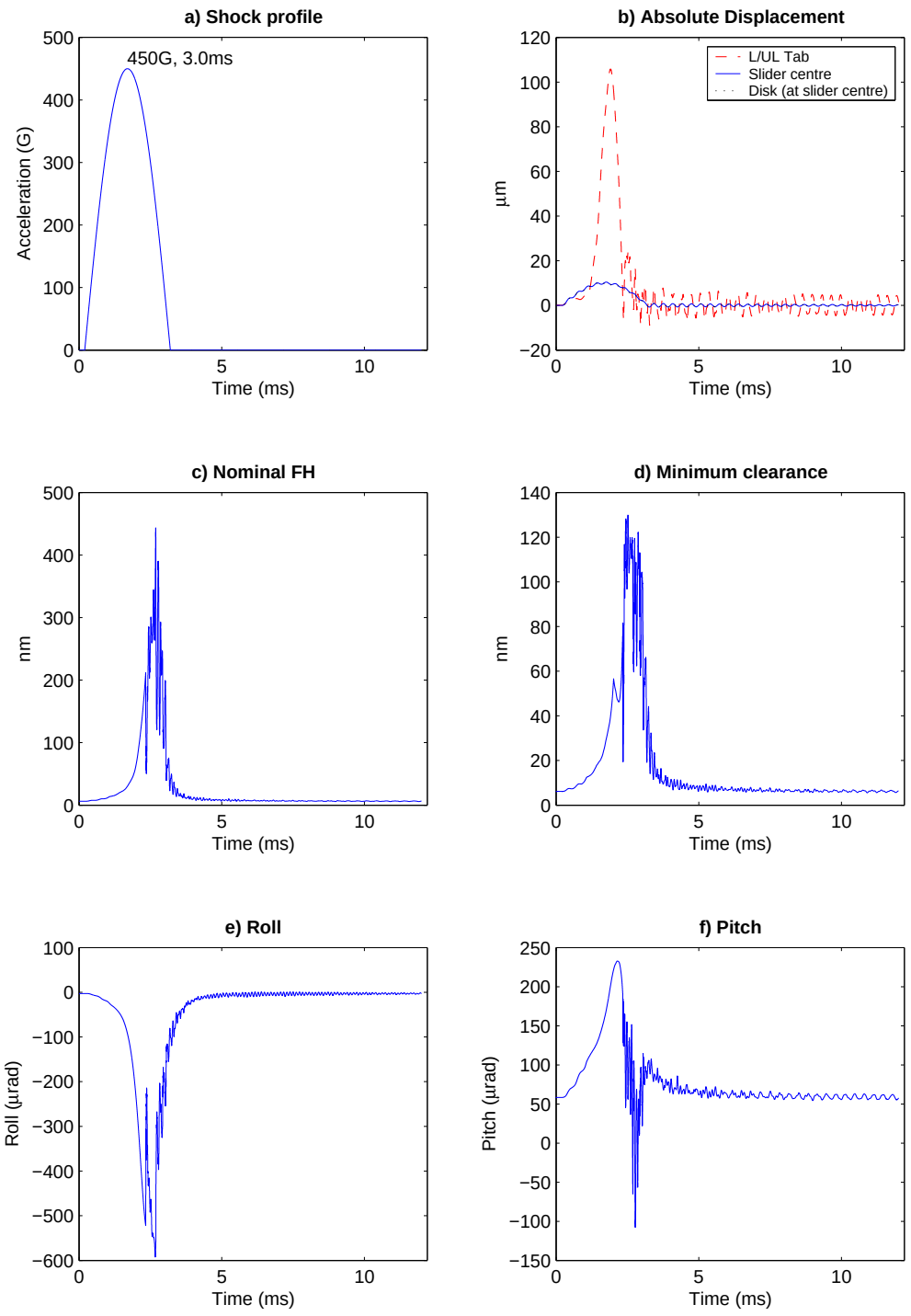

Figure 23: Slider Response for 450G, 3.0 ms shock

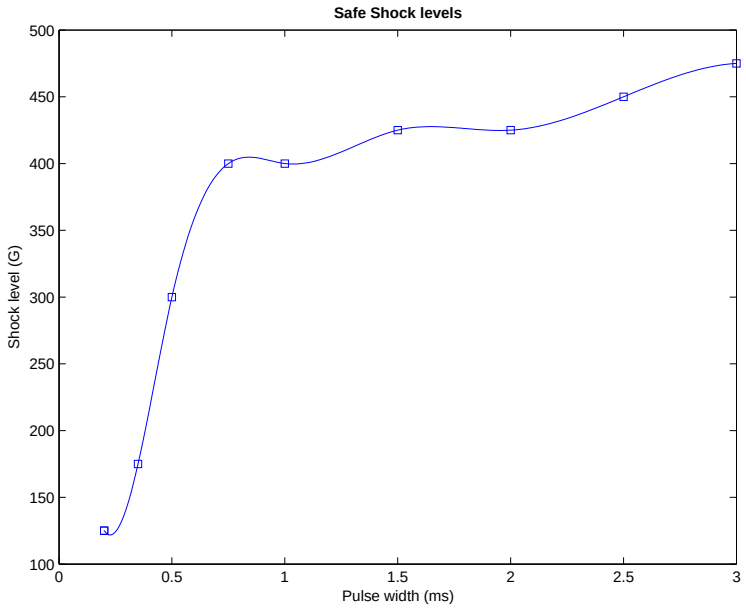

Figure 24: Safe shock levels for varying pulse widths